





ORIGINAL RESEARCH ARTICLE

Valorization of Spent Plastics for Hydrocarbon Production with Improved Economic Worth and Environmental Remediation: A Pre-degradation Approach

Amina Muhammad Mustapha^{1*}, Victor Ugbetan Agbogo², Ibrahim Mohammed Inuwa¹ and Moses Titus Yilleng³.

¹Department of Pure and Applied Chemistry, Faculty of Physical Sciences, College of Science, Engineering and Computing, Kaduna State University, PMB 2339, Kaduna, Nigeria.

²Department of Chemistry, Faculty of Natural and Applied Science, Nigerian Army University, PMB 1500, Biu, Borno State, Nigeria.

³Department of Chemistry, Faculty of Natural Sciences, University of Jos, PMB 2084, Plateau State, Nigeria.

ABSTRACT

Amidst the world's energy crisis, our society faces a growing environmental dilemma as plastic junk winds up in landfills and bodies of water, infiltrating the food chain. In Nigeria, water packaged in transparent low-density polyethylene (LDPE) sachets is widely consumed by the populace and the sachets are discarded in large quantities. Waste LDPE was subjected to pyrolysis, which involves first dissolving it in toluene and then degrading it using a modified zeolite catalyst. ZSM-5 underwent modification with the addition of nickel using the hydrothermal technique. The catalyst and pure zeolite's elemental composition, surface area, crystal structure, and morphology were examined through Energy Dispersive X-ray (EDX) analysis, Brunauer-Emmett-Teller (BET), X-ray diffraction (XRD) and Scanning Electron Microscopy (SEM), respectively. The liquid products were characterized using Fourier Transform Infrared Spectroscopy (FTIR) and Gas chromatography-mass spectrometry (GC-MS). The result showed a high yield of liquid products ($\approx 72\%$) rich in alkene, a valuable gasoline blending stock that can be used as a feedstock for various chemical processes. The physicochemical parameters of the oil obtained via both thermal and catalytic cracking were also determined and it was observed that the product of the catalyzed process had better properties with some of the oil-fuel characteristics obtained fitting perfectly within the range of standard fuel. Dissolving the LDPE in toluene reduced its viscosity, allowing for easy handling and uniform heating within the reactor. Furthermore, the dissolution method before degrading could help prevent pipelines from getting stuck with melted plastic feed if plastic waste conversions through cracking are scaled up to continuous operations.

ARTICLE HISTORY

Received April 25, 2024.

Accepted June 28, 2024.

Published July 03, 2024.

KEYWORDS

Plastic waste, Zeolite, Valorization, Physicochemical parameters, Energy



© The authors. This is an Open Access article distributed under the terms of the Creative Commons Attribution 4.0 License (<http://creativecommons.org/licenses/by/4.0>)

INTRODUCTION

The rapid economic development has led to a surge in the demand and production of plastic worldwide. As a result, our society is facing an ever-increasing environmental problem since plastic garbage is not biodegradable and ends up in waste sites and waterbodies, where it impacts the health of wildlife, especially in marine areas, and also poses threats to human health (Rouch, 2021). According to the UNIDO (2021), Nigeria ranks ninth on the list of countries with the highest contributions to plastic pollution globally, with over 88% of the plastic waste generated not recycled. One of the major plastic wastes in Nigeria is the transparent low-density polyethylene (LDPE) widely used to package sachet water consumed by the populace and large quantities of these sachets are thrown away everywhere.

Various renewable energy types were developed by researchers to combat the energy crisis, and the ones that were adapted to national grids received government rewards through feed-in tariff systems in multiple countries (Wong *et al.*, 2015). Due to the increasing demand for plastic-made consumer products and the energy crisis problem, there is an urgent need to propose proper alternatives to plastic waste disposal to minimize pollution, create more energy sources, and simultaneously create wealth. Among the proposed solutions: enzymatic degradation (Kaushal *et al.*, 2021), plastic-to-fuel conversion (Li *et al.*, 2022), mechanical recycling (Schyns and Shaver, 2020), microbial degradation (Shilpa *et al.*, 2020), amidst others, catalytic cracking seems to be an

Correspondence: Amina Muhammad Mustapha. Department of Pure and Applied Chemistry, Faculty of Physical Sciences, College of Science, Engineering and Computing, Kaduna State University, PMB 2339, Kaduna, Nigeria. ✉ amina.mustapha@kasu.edu.ng. Phone Number: +234 803 805 8757.

How to cite: Mustapha, A. M., Agbogo, V. U., Inuwa, I. M., & Yilleng, M. T. (2024). Valorization of Spent Plastics for Hydrocarbon Production with Improved Economic Worth and Environmental Remediation: A Pre-degradation Approach. *UMYU Scientifica*, 3(3), 16 – 30. <https://doi.org/10.56919/usci.2433.003>

interesting option since it converts plastic waste into liquid fuel.

Numerous research reports have indicated polymer pyrolysis and cracking as solutions for the disposal of these plastic wastes after their consumption. These processes have shown the depolymerization of plastic waste into smaller hydrocarbons in liquid and gaseous forms that could be used as fuels (Burange *et al.*, 2014). Different catalysts have been employed by researchers for the conversion of plastics to fuels, including activated carbon (Sarker *et al.*, 2013; Bai *et al.*, 2022), clays (Seliverstov *et al.*, 2022; Mibei *et al.*, 2023), metal oxides (Kholidah *et al.*, 2018; Ethiraj *et al.*, 2022), and carbonates (Kunwar *et al.*, 2016). Pre-degradation of LDPE in a suitable solvent before pyrolysis reduces the resident time

(Wong *et al.*, 2016), coupled with the fact that the use of a fixed bed reactor enables the easy determination of the polymer conversion based on the weight of the unreacted polymer in the reactor after the cracking process. Zeolites have become a popular choice for catalysts in polymer pyrolysis and cracking because of their improved catalytic properties over those of other catalysts (Mark *et al.*, 2020; Li *et al.*, 2023; Liu *et al.*, 2023), and it has been shown that when metals are injected into zeolites, the pyrolysis of polymers yields higher-quality liquid products (Yao *et al.*, 2018; Akubo *et al.*, 2019; Quesada *et al.*, 2020) as well as pyrolysis of biomass (Vichaphund *et al.*, 2014). This study employed a pre-degradation approach to polymer pyrolysis using a modified zeolite catalyst to explore the catalyst's activity and the properties of the products obtained.

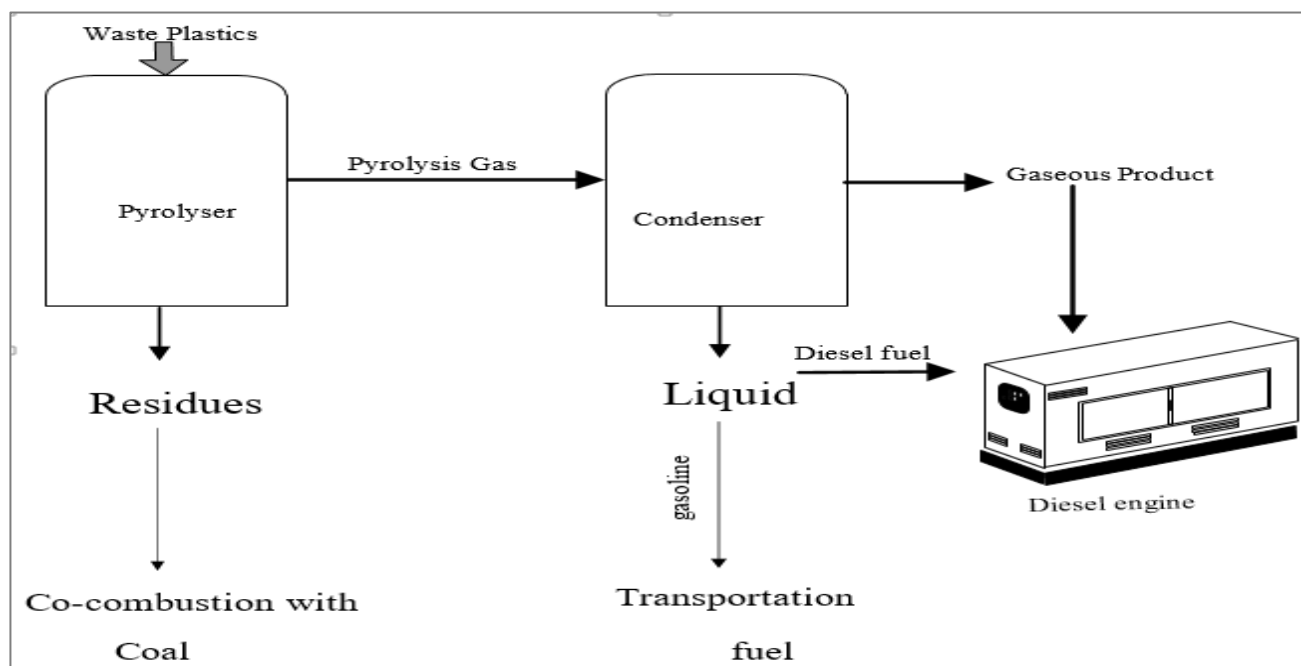


Figure 1: A schematic diagram of the proposed system for converting waste plastics into fuels.

MATERIALS AND METHOD

Chemicals and Reagents

All compounds were used without further purification; they were all bought from Sigma-Aldrich in Germany. ZSM-5, methanol (CH₃OH), toluene (C₇H₈), nickel (II), nitrate hexahydrate (Ni (NO₃)₂.6H₂O), and methanol were the chemicals employed in this work.

Synthesis and characterization of Ni-ZSM-5 catalyst

Nickel modified zeolite (Ni-ZSM-5) of 10wt% Ni composition was developed by hydrothermal method using modified procedures by Yao *et al.* (2018). 5.50 g of Ni (NO₃)₂.6H₂O was dissolved completely in 100 ml of methanol to form solution A, and 10.0 g of ZSM-5 (ZA) was added to 25 ml of deionized water with stirring to form solution B. Using a magnetic stirrer set at 50 rpm, these two solutions were homogenized for three hours at

29°C. The slurry was further heated for 12 hours at 500°C and placed inside an autoclave lined with Teflon. Filtration was done when the autoclave was allowed to cool to ambient temperature.

The filtered precipitates were allowed to cool and then pulverized in an agate mortar and pestle after being dried at 120°C for two hours at 100°C. Following three hours of calcination at 550 °C, the ground sample was allowed to cool before being placed in an airtight container for further examination. This sample was named Z_B. The produced catalyst and pure zeolite were characterized for surface area, crystal structure, morphology and elemental content. The textural qualities were determined using Autosorb-1-C (Quantachrome Instrument Corp.) and N₂ adsorption and desorption at liquid nitrogen temperature (196oC). NOVA 2200e instrument was utilized to determine the specific surface area with the Brunauer–

Emmett–Teller (BET) method. The Barrett–Joyner–Halenda (BJH) method measured the pore size distribution. Utilizing a Rigaku D/max 2550PC system with $\text{CuK}\alpha$ radiation, X-ray diffraction (XRD) measurements were performed, the morphology was determined using a Scanning Electron Microscope (FEI Quanta 250), and energy dispersive X-ray (EDX) analysis was used to determine the elemental composition.

Feedstock for pyrolysis

The polymer used was low-density polyethylene waste (used water sachets) collected from a waste vendor in Danbushiya, Millennium City, Kaduna State. The spent

LDPE was dissolved in hot toluene to produce an LDPE-toluene solution. The dissolution procedure was adopted from Wong *et al.* (2014) with a slight modification.

LDPE Waste Cracking

Pyrolysis experiments were carried out using a batch reactor. The schematic diagram of the experimental apparatus is shown in Figure 2. The pyrolyzer was made of stainless steel and covered with heaters. The pyrolyzer's inner diameter and height were 50 mm and 200 mm, respectively. A double-tube condenser was installed at the outlet of the pyrolyzer to separate gas and liquid products.

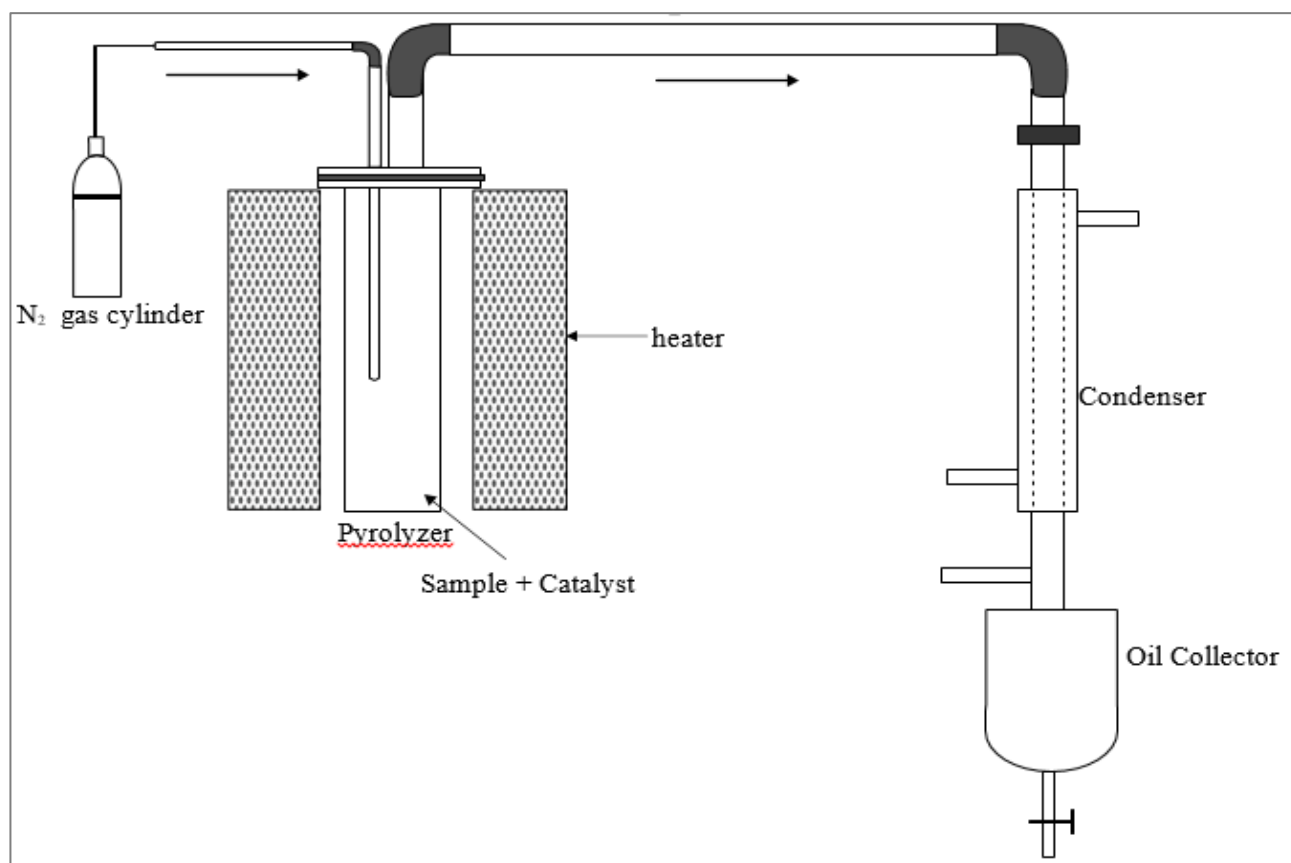


Figure 2: A schematic diagram of the experimental apparatus.

In these experiments, LDPE-Toluene solution was fed into the pyrolyzer, where the solution was heated and then volatilized into the condenser. The nitrogen gas flow rate was 100 ml min^{-1} . After the pyrolysis reaction, the gas was cooled in the condenser to recover liquid products. The Liquid products were then collected and weighed for the mass balance calculation. The remaining solids deposited in the pyrolyzer were defined as the residue. The experiments were carried out at a pyrolyzer temperature of 500°C . Experiments using similar conditions but in the presence of Ni-ZSM-5 catalyst (2 g, 4 g, and 8 g) were also conducted for comparison. The equations involved were as follows:

$$\text{LY} = M_1 / M_i \times 100 \% \quad (1)$$

$$\text{SY} = M_2 / M_i \times 100 \% \quad (2)$$

$$\text{GY} = 100 \% - (\text{LY} + \text{SY}) \quad (3)$$

where LY, SY, GY were the yields of oil, solid products and gas after pyrolysis, respectively. M_i was the mass of LDPE-Toluene solution, M_1 and M_2 were the mass of liquid and solid products after pyrolysis.

RESULTS AND DISCUSSION

Catalyst Characterization

Brunauer Emmet and Teller (BET) nitrogen adsorption analysis was used for the determination of surface area,

pore size, and pore volume of the pure and modified catalysts. Table 1 below shows the surface area and porosity of the pure and modified catalysts. The impregnation with the metal decreased surface area per unit mass. Akubo *et al.* (2019) also reported a small decrease in the surface of the Y-zeolite catalyst when impregnated with metal promoters.

Table 1: Textual properties of the pure and modified catalysts

Samples	Ni loading (wt %)	BET surface area (m ² /g)	Total pore volume (cm ³ /g)	Average pore diameter (nm)
ZSM-5	0	223.18	0.125	2.131
Ni-ZSM-5	10	136.84	0.076	2.133

XRD analysis was carried out to identify the components and crystallinity of the catalysts. Figures 3a and 3b represented XRD patterns of ZSM-5 and Ni-ZSM-5,

respectively. Based on the X-ray diffraction pattern for Z_A, peaks at 2θ = 7.2°, 10.0°, 13.3°, 16.4° and 22-34° were observed. These peaks correspond to specific crystallographic planes within the MFI structure, which match the reference pattern for the MFI framework in ZSM-5 zeolites (JCPDS no. 44-0003) (Huang *et al.*, 2015). The sharp and intense peaks indicate a high degree of crystallinity in the sample. The modified catalyst showed reflections at 44.1° and 53.7°, corresponding to metallic nickel (Wong *et al.*, 2016). Compared with the fresh (parent) zeolite, the peaks in Z_B were present at the same 2θ values but were less intense. This observation shows a minor decrease in the impregnated zeolites' crystallinity due to the nickel impregnation, which led to distortions in the regular crystalline framework of the zeolite as a result of the amorphous phases or non-crystalline domain formation within the zeolite structure. This is consistent with the findings of Wong *et al.* (2016) and Huang *et al.* (2016).

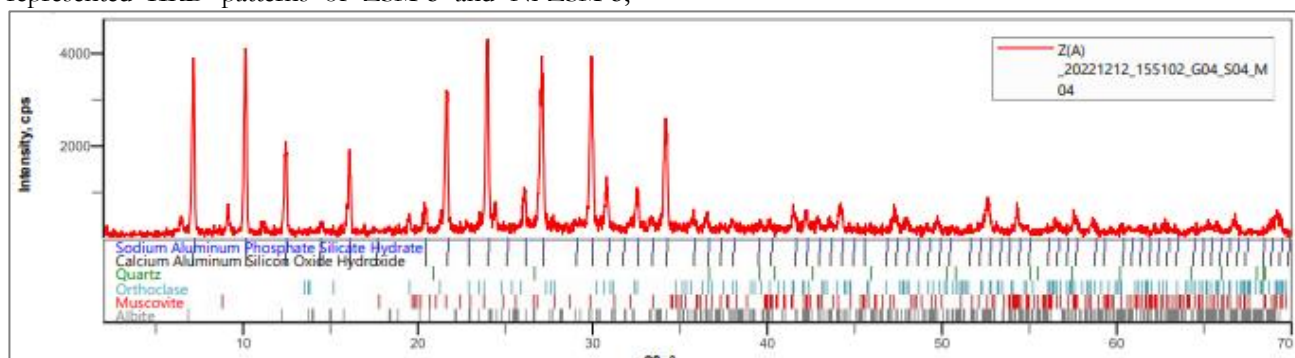


Figure 3a: X-ray diffraction profile of the fresh zeolite (Z_A)

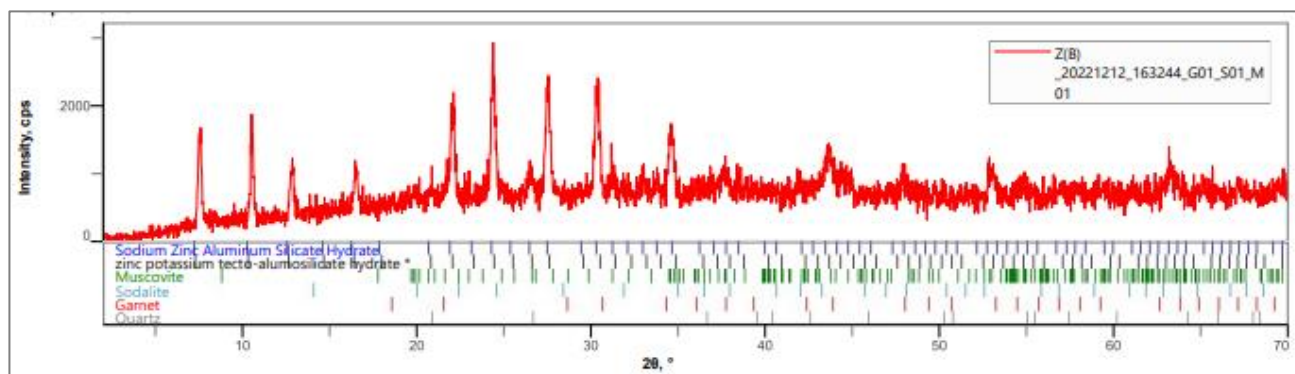


Figure 3b: X-ray diffraction profile of the Ni-ZSM-5 (Z_B)

The SEM images of pure ZSM-5 zeolite before and after nickel impregnation are shown in Figures 4a and 4b. It can be observed from Figure 4a that the particles appear to be clustered together, which is common for zeolite powders. The surface of the particles appears rough, irregular-shaped, and vary in size. Figure 4b shows a collection of rough-surfaced particles irregularly shaped and clumped together. Because Nickel (Ni) has a higher atomic number (28) than aluminum (13) and silicon (14), which are the main components of zeolites, areas where nickel is concentrated would be expected to appear brighter in the BSD image mode (Nanakoudis, 2019). This suggests that the nickel may be dispersed in different regions throughout the zeolite particles. Nickel dispersion

in the modified zeolite is evident from the EDX spectrum (Figure 5b).

ZSM-5 is an aluminosilicate zeolite, meaning its framework is built from aluminum (Al), silicon (Si), and oxygen (O) atoms, and as expected, prominent peaks corresponding to Al, Si, and O were observed on the EDX spectrum. Traces of elements such as sodium (Na), nitrogen (N) and carbon (C) were also observed (Figure 5a). For the modified ZSM-5 (Z_B), a peak corresponding to nickel (Ni) was observed in addition to the peaks observed on the EDX spectrum of pure ZSM-5 (Z_A) (Figure 5b). The elemental composition for both ZSM-5

and Ni-ZSM-5 are depicted in Table 2. This confirms the successful modification of the Z_A with nickel. The height of each peak is roughly proportional to the relative abundance of that element in the sample. A higher peak indicates a greater concentration of that element, which aligns with the values in Table 2. The differences in atomic concentrations of similar elements in the two samples resulted from ion exchange and substitution, which resulted from doping with nickel, replacing other elements and variations of atomic concentrations within the framework compared to the pure zeolite. Also, the non-uniform distribution of the dopant within the zeolite structure may lead to localized regions where the concentration of nickel and potentially other elements varies significantly compared to the pure zeolite.

Effect of Catalyst dose on product composition

The effectiveness of Ni-ZSM-5 catalysts at various dosages on the catalytic conversion of LDPE was compared (Figure 6a). The amount of catalyst employed had a major impact on the yield distribution. The yield of solids dropped significantly while the output of gas and oil increased significantly with the increase in catalyst mass. This could be because of the breakdown and secondary reaction of the volatiles produced during the pyrolysis of LDPE (Zhang *et al.*, 2018). The yield of gas grew significantly, the yield of solids increased little, and the yield of oil decreased significantly as the catalyst dose increased.

Figure 6a illustrates that the liquid phase yield was marginally lower at 2 g (51.6%) and higher at 4 g (71.6%) of catalyst mass. As catalyst mass rose further, the percentage of the polymer converted into a liquid product decreased (38.7%), and the gaseous component increased. The catalyst dose increase allows for the weakening of the chain structure and the breaking of additional polymer chains, which results in the formation of smaller hydrocarbons in the form of gaseous compounds (Wong *et al.*, 2017; Roozbehani *et al.*, 2015). Heavier chemical cracking is also possible with ZSM-5 because of its bigger intracrystalline pore structure and smaller pore size. The catalyst's inner cavity can be reached by diffusion from the first degradation sample on its outer surface, which leads to extremely high gas yields upon further breakdown into gaseous components (Song *et al.*, 2021).

The yields for liquid, gas, and solid were comparable for the three runs conducted in the thermal pyrolysis step. Figure 6b illustrates no discernible variation in gas yield among the three runs (42.0 %, 41.2 %, and 40.9 %). Except for the instance whereby an 8 g catalyst dose was employed, these gas yields were greater than the catalytic runs. Additionally, the residue produced in the thermal runs was, on average, higher than that of the catalytic pyrolysis, and the liquid product from the catalytic pyrolysis (using 4 g) was much higher than that obtained from all of the thermal runs. This result is consistent with the works of Setiawan *et al.* (2021), who also obtained a higher percentage of gases in the thermal pyrolysis of LDPE.

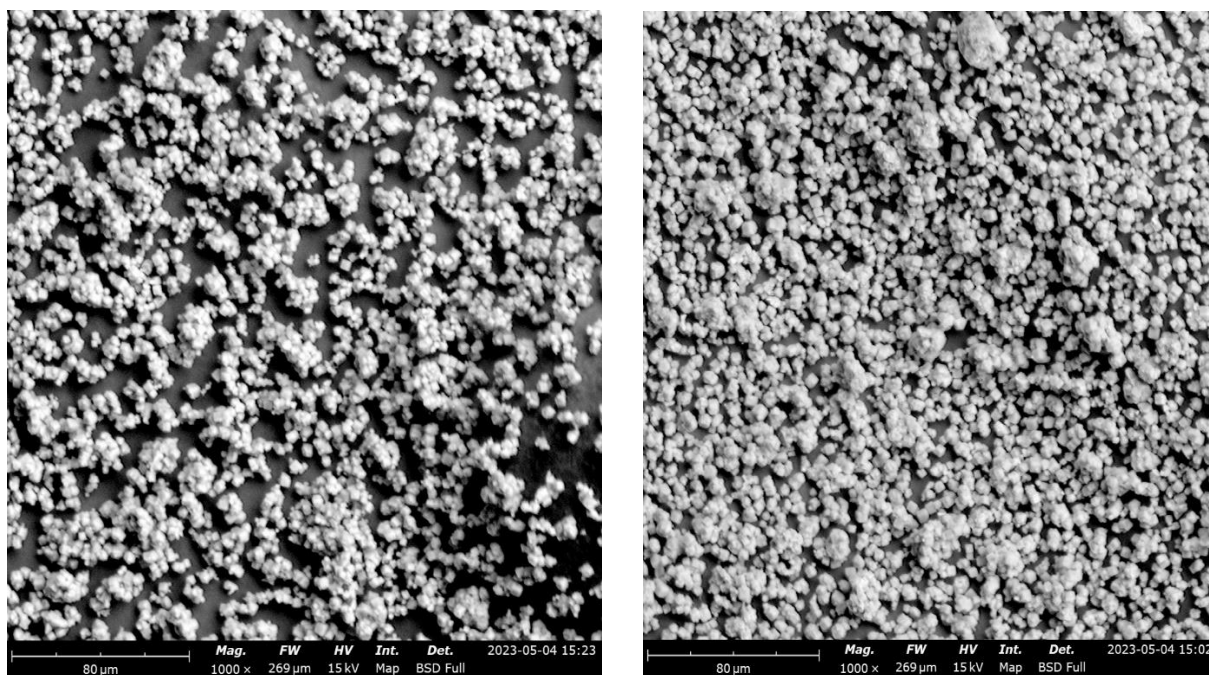
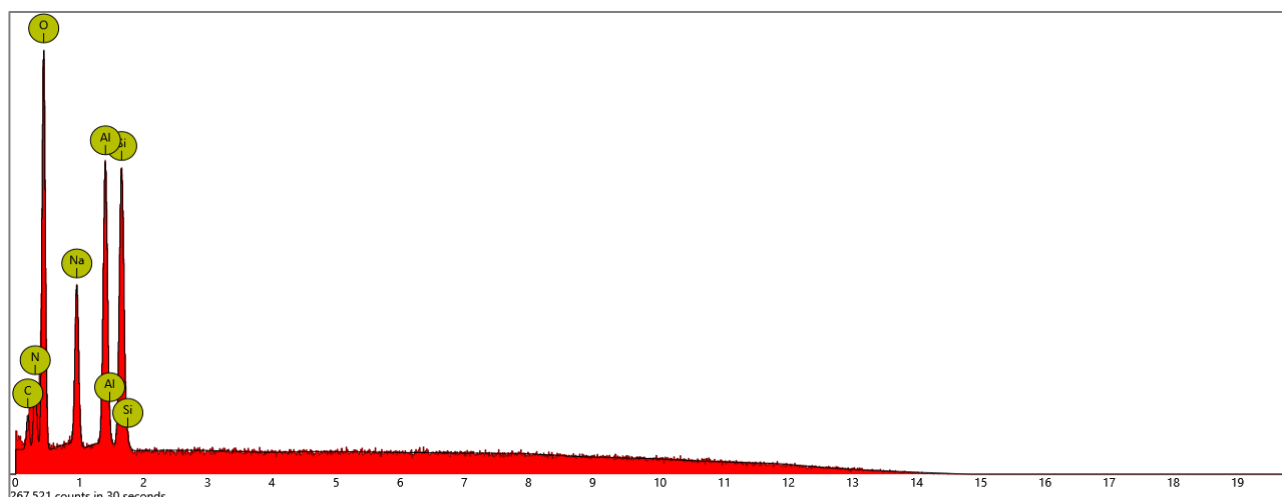
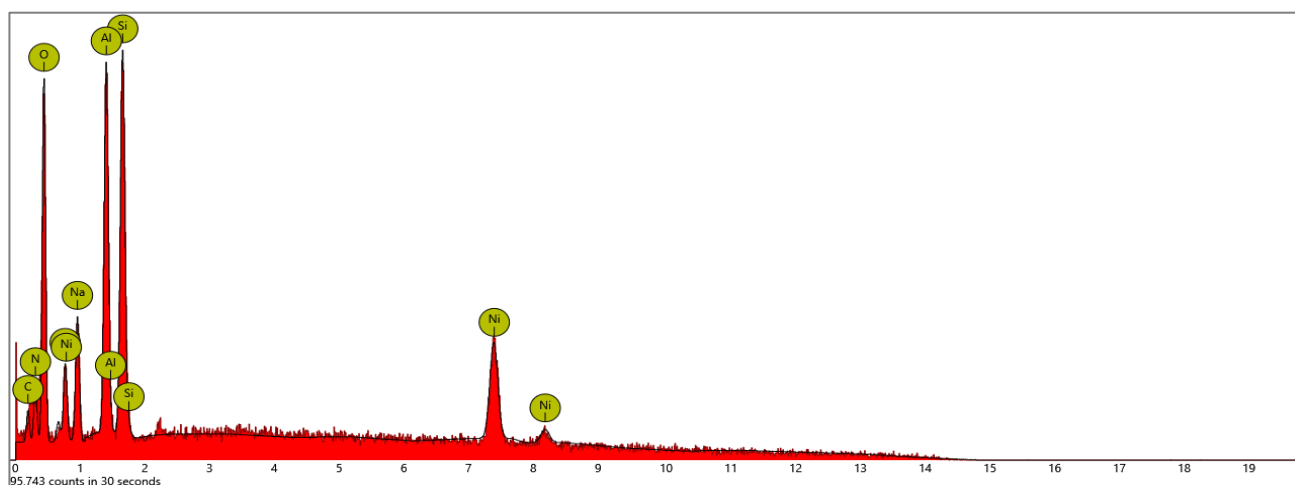


Figure 4 (a: left and b: right): Scanning electron microscopy (SEM) images of (a) Z_A and (b) Z_B samples.

Table 2: The elemental composition for both ZSM-5 and Ni-ZSM-5

ZSM-5 (Z _A)				Ni-ZSM-5 (Z _B)			
Element Number	Element Symbol	Atomic Conc.	Weight Conc.	Element Number	Element Symbol	Atomic Percentage	Weight Percentage
8	O	60.20	51.59	8	O	47.75	32.72
11	Na	11.77	14.50	11	Na	10.65	10.48
13	Al	9.76	14.11	13	Al	12.65	14.62
14	Si	8.34	12.54	14	Si	11.15	13.41
7	N	8.16	6.12	7	N	6.78	4.07
6	C	1.77	1.14	6	C	1.50	0.77
				28	Ni	9.52	23.93


Figure 5a: EDX Peaks in ZSM-5 (Z_A)

Figure 5b: EDX Peaks in Ni-ZSM-5 (Z_B)

Fourier Transform Infrared Spectroscopy of thermally cracked and catalytically cracked fuel oil

FTIR analysis of the thermal pyrolysis of the waste LDPE reveals key information about the resulting products. Peaks around 3096 cm^{-1} (strong C-H stretch) indicate abundant aliphatic hydrocarbons, fuel's main constituents. Weak peaks around $1605\text{--}1450\text{ cm}^{-1}$ are attributed to the stretching vibrations of aromatic ring C=C bonds. This is consistent with the work of [Doğan and Kayacan \(2008\)](#), who observed a weak peak in this region, indicating a low concentration of aromatic species in their liquid product. Peaks around $1750\text{--}1690\text{ cm}^{-1}$ reveal the presence of

oxygen-containing compounds (aldehydes, ketones, and alcohols), which might influence combustion behaviour ([Figure 7a](#)).

FTIR analysis of the oil obtained from the catalytic pyrolysis of waste low-density polyethylene (LDPE) using nickel-impregnated ZSM-5 provides valuable insights into the effectiveness of the catalyst and the nature of the products formed. The peak at 2977 cm^{-1} indicates C-H stretching vibrations in alkanes. The peak at 2160 cm^{-1} indicates C=C stretching vibrations in alkenes. Peaks around 1720 cm^{-1} indicate the presence of carbonyl groups (C=O), potentially from ketones or aldehydes.

The presence of bands around 1605 and 1500 cm^{-1} (aromatic C=C stretching) suggests the presence of aromatic rings in the liquid product. This is in line with studies that showed that Ni-ZSM-5 catalysts can promote aromatics formation during LDPE pyrolysis. Weaker peaks around 880 and 790 cm^{-1} might suggest trace aromatics (Figure 7b). These are desirable fuel components due to their high energy density and impact

on fuel quality. Studies have shown a significant increase in these bands compared to non-catalytic pyrolysis (Wong *et al.*, 2017; Kim *et al.*, 2017). Decreased aliphatic bands indicate the efficient breakdown of long-chain LDPE molecules into smaller aliphatic hydrocarbons (e.g., alkanes, alkenes). Several studies reported significant intensity reductions in bands corresponding to aliphatic hydrocarbons (Wong *et al.*, 2017; Barzallo *et al.*, 2023).

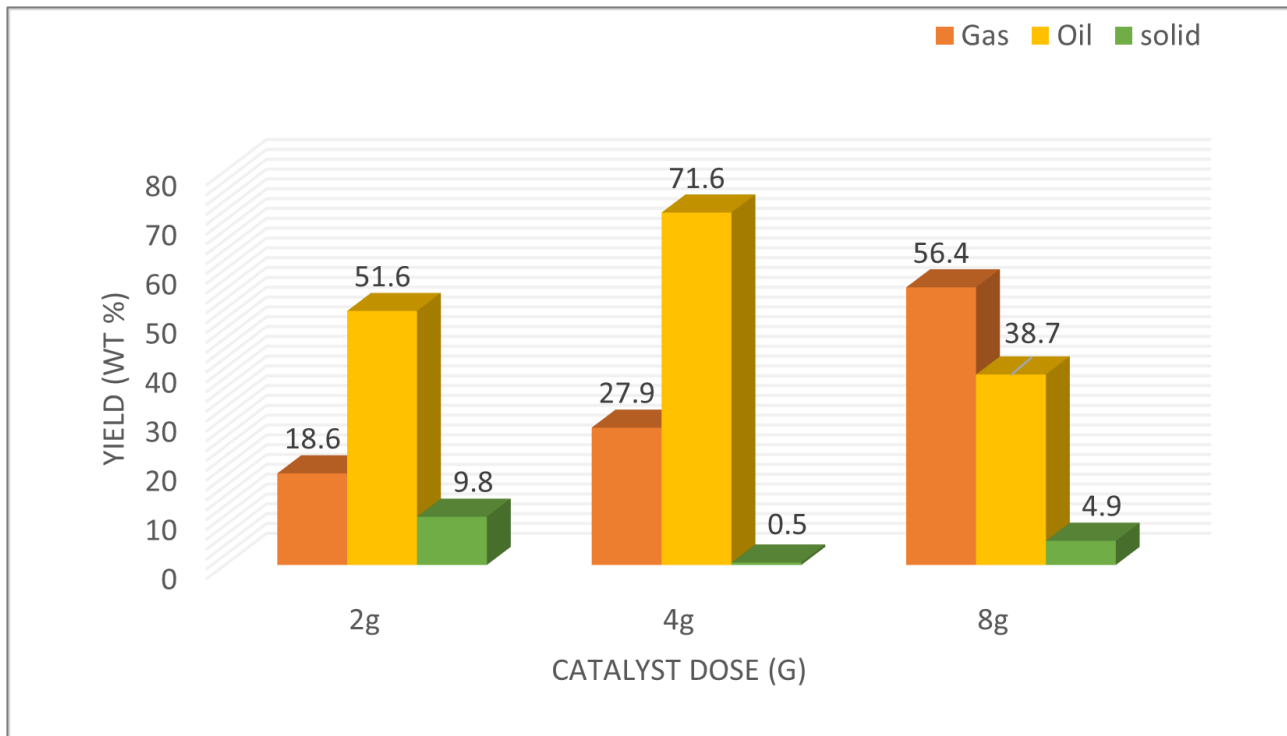


Figure 6a: Three-phase yield diagram of LDPE pyrolysis using Ni-ZSM-5 catalyst

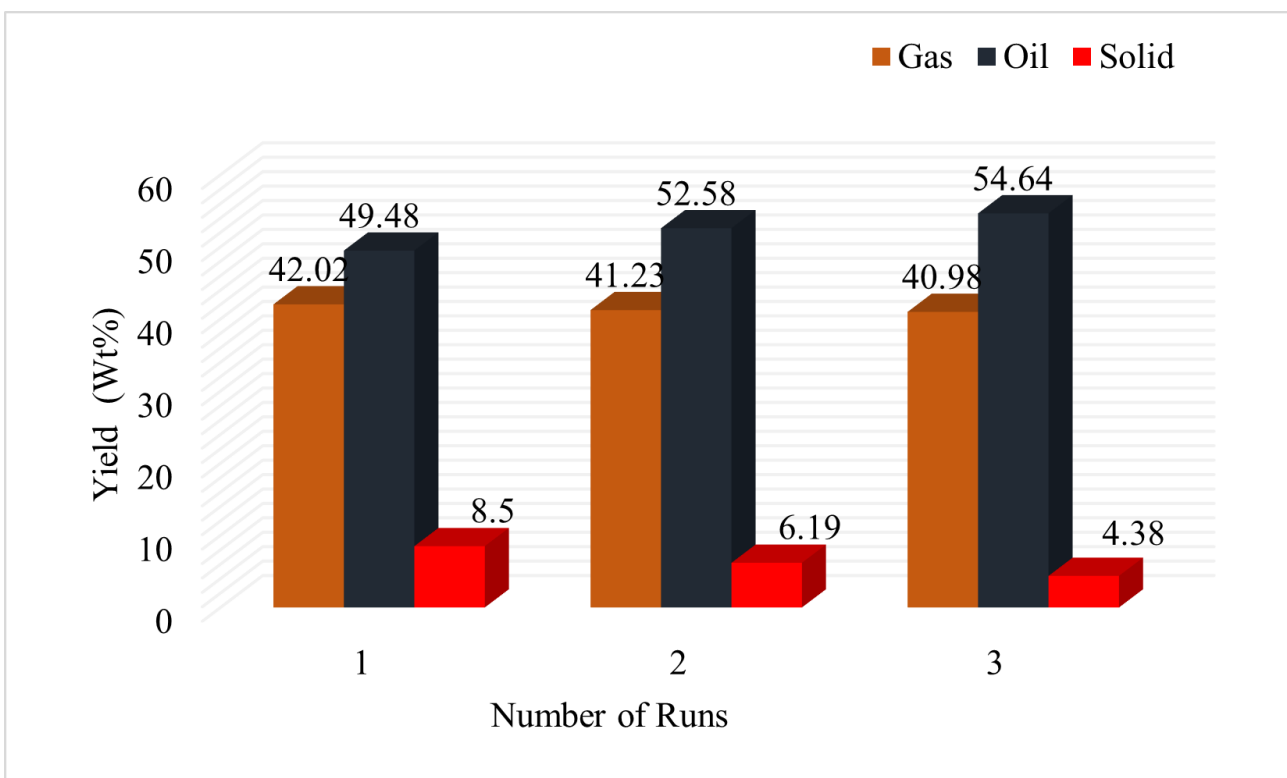


Figure 6b: Three-phase yield diagram of LDPE pyrolysis without catalyst

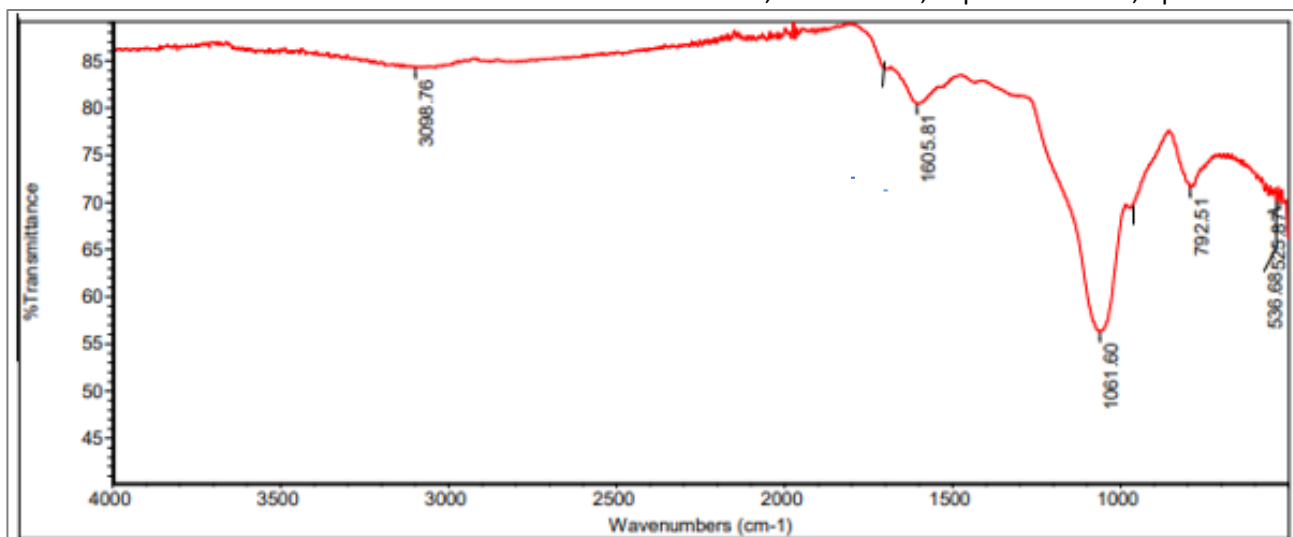


Figure 7a: FTIR spectrum of the oil obtained from the thermal pyrolysis of waste LDPE

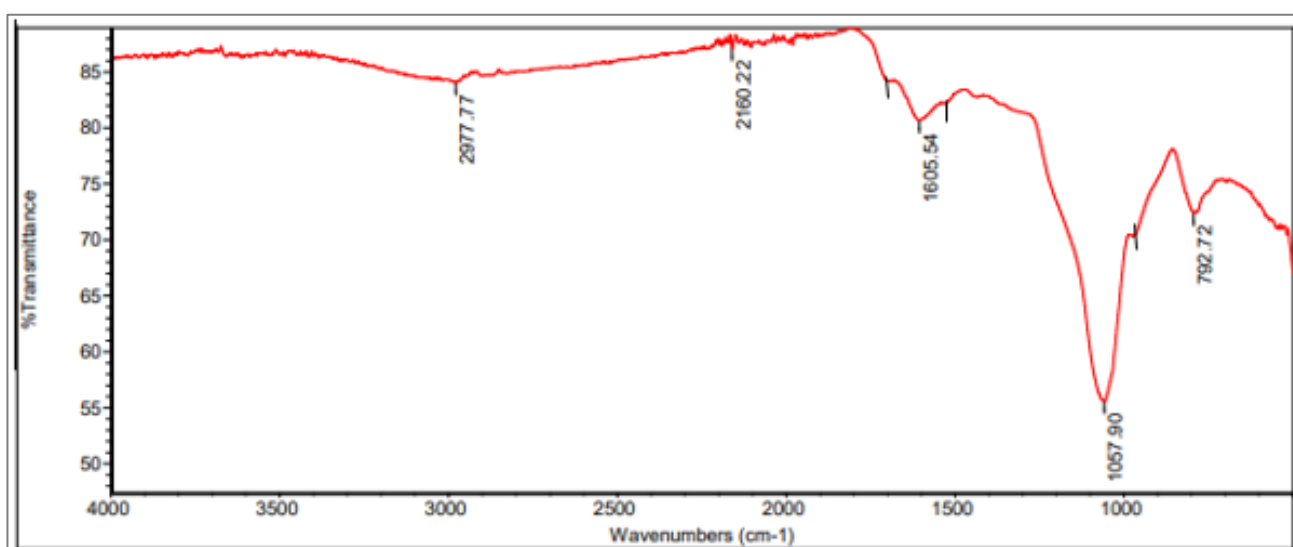


Figure 7b: FTIR spectrum of the oil obtained from the catalytic pyrolysis of waste LDPE

The Gas Chromatography-Mass Spectrometry of the Liquid Products

The GC-MS analysis of the liquid products obtained from the thermal and catalytic pyrolysis of LDPE are presented in Table 3 and Table 5 (see appendix), respectively, while their respective compositions are presented in Table 4 and Table 6. The Liquid products from the thermal pyrolysis showed 53 peaks with the percentage compositions of Alkanes (25.67 %), Alkenes (1.48 %), Aromatics (23.40 %), and other components (49.45 %). The Liquid products from the catalytic pyrolysis showed 85 peaks with the percentage compositions of Alkanes (11.41 %), Alkenes (53.45 %), Aromatics (4.48 %), and others (30.66 %). It was observed that the products obtained from catalytic pyrolysis have a much higher percentage of olefins and a lower percentage of heavier alkanes and aromatics, while that of thermal pyrolysis possesses a higher percentage of alkanes and aromatics and a lower percentage of alkenes. Strong Brønsted acid sites within the zeolite framework promote cracking reactions that favor alkene formation. These sites act as proton donors,

breaking down the long hydrocarbon chains of LDPE into alkenes. Studies have shown that Zeolites with a high concentration of Brønsted acid sites lead to a higher alkene yield in the liquid products (Agulló *et al.*, 2007; Hasan *et al.*, 2022).

Furthermore, the pore size of the zeolite can influence the selectivity towards alkenes. Zeolites with medium pore sizes, like ZSM-5, are ideal for promoting alkene formation (Budsareechai *et al.*, 2019). This finding is also consistent with Li *et al.* (2018) and Rajan *et al.* (2023), whose results showed that all the zeolite catalysts significantly reduced aromatics yield and increased alkenes yield. The low alkane (11.41%) and aromatic (4.48%) content further strengthens the effectiveness Ni-ZSM-5 in suppressing these products and promoting alkene formation.

The presence of fluorine atoms in some components of the liquid products could result from the incorporation of fluorinated compounds in the plastics for improved properties like slip or water repellency. These additives

may degrade during pyrolysis, generating fragments that GC-MS then identifies in the liquid product.

Table 4: Liquid product composition of thermal pyrolysis of LDPE

S/N	Component	Respective percentages (%)
1	Alkane	25.6682
2	Alkene	1.47920
3	Aromatics	23.4033
4	Others	49.4493
	Total	100

Table 6: Liquid product composition of catalytic pyrolysis of LDPE

S/N	Component	Respective percentages (%)
1	Alkane	11.4095
2	Alkene	53.4495
3	Aromatics	4.4811
4	Others	30.6599
	Total	100

Fuel properties of pyro oil

The refinery's middle distillates - diesel and gasoline - and the pyro oil have comparable qualities. Table 7 provides an overview of the physicochemical characteristics of the oil as determined by the ASTM. Specific gravity and density are two factors that are crucial for fuel quality control. The pyro oil produced by thermal and catalytic pyrolysis of waste low-density polyethylene (LDPE) has specific gravity and density values within normal ranges for fuel oils (Table 7). Fuel's tendency or reluctance to flow, governed by its viscosity and kinematic viscosity, is one of its fundamental properties. The study's results are within the range of diesel fuel. High viscosity increases engine temperature, fuel consumption rate, and friction, according to Ahmad *et al.* (2015).

In that order, the pyro oil derived from the two pyrolysis processes had pH values of 6.1 and 5.7. Generally speaking, fuel oil should be between 5.5 and 6.5 (ASTM D4739). Both of these values are within this range. The fuel oil produced through catalytic pyrolysis has a lower pH, and this is because the zeolite catalyst is acidic, which encourages cracking reactions using proton transfer mechanisms. Barzallo *et al.* (2023) state that these reactions produce low-molecular-weight organic acids and acidic byproducts such as olefins, phenols, and aromatics with sulfonic acid groups.

Moreover, particular cracking reactions during each step might also affect pH. Thermal homolysis, which cleaves bonds without adding new functional groups, is the main process of thermal cracking. By contrast, a variety of processes, such as isomerization, dehydrogenation, and alkylation, may be involved in catalytic cracking, which may result in the introduction of acidic functional groups such as olefins and carboxylic acids (Wong *et al.*, 2017).

A fuel's flash point is the lowest temperature at which enough vapor is produced to create an airborne flammable combination. For a given material, handling one with a greater flash point is safer than the other. Spent low-density polyethylene (LDPE) was pyrolyzed thermally and catalytically to create pyro oil, with a flash point of 96.8°C and 112.3°C. With a flash point of 112.3°C, the catalytically generated oil was slightly higher than the usual diesel temperature range of 52 - 96°C. Higher flash point fuels can be handled and stored more safely, especially in warmer climates.

For this reason, fuel oil produced by thermal and catalytic pyrolysis can be handled and stored safely. In contrast, fuels with lower flash points tend to be more volatile, and in some situations, they may ignite more quickly and vaporize more easily (ASTM D56). The pour point is the temperature at which oil loses its flow characteristics. The pour point of thermal and catalytic generated oil was slightly higher (1.4 and -5.3°C) than that of standard fuel (-9.2°C). High-pour-point fuels need not be utilized in cold climates (Damodharan *et al.*, 2019) because they can solidify or gel-like, making it impossible to pump into the engine or transport efficiently.

The refractive index of fuel oil often rises when heavier hydrocarbons and aromatic compounds are present. The refractive indices of the pyro oil generated from the thermal and catalytic pyrolysis of leftover LDPE were 1.48 and 1.52, respectively. Middle distillates have refractive indices between 1.42 and 1.49. Fuel oil with a higher refractive index might include more aromatics or heavier molecules than fuel oil with a lower value. Aromatics can improve combustion efficiency and cetane number, but they can also raise the emissions of a number of undesirable pollutants (ASTM D1218). This further implies that the thermally and catalytically broken LDPE contains heavy components.

Waste LDPE was pyrolyzed thermally produced pyro oil with a heating value of 32.22 MJ/kg and 42.11 MJ/kg using catalytic pyrolysis. Both fall within the approved 41–46 MJ/kg range for diesel fuel. This number is consistent with Das and Tiwari's (2018) investigation of the physicochemical properties of oil derived from plastic via slow pyrolysis. According to the IEA (2023), fuel having a high heating value produces more heat per unit volume, which may lead to lower fuel consumption for the same heating demand and potentially even lower fuel prices overall. In addition, certain fuel oils with higher heating values have lower sulfur content, which results in less emissions, whereas fuels with lower heating values have higher sulfur content, which produces more pollutants. Therefore, the former offers greater advantages when comparing the heating value of the fuel with HV42 to that of the oil produced from thermally pyrolyzed waste LDPE with HV of 32.

Considering the high alkene content of the liquid product, one possible application for it would be as a valuable gasoline blending stock. The octane rating of gasoline is

one property that alkenes can enhance. Yet, to satisfy particular fuel requirements, additional processing or blending with regular gasoline might be required. Additionally, various chemical processes could use the

alkene-rich result as a feedstock. Alkenes are necessary building blocks for many compounds, such as polymers, detergents, and lubricants.

Table 7: Physicochemical analysis on thermally and catalytically (4g cat.) pyrolyzed oil sample in accordance to ASTM D6751

S/N	Properties	LDPE thermal Oil	LDPE Cat Oil	Standard values for diesel fuel
1	Specific Gravity (@ 30°C)	0.844	0.868	0.82 – 0.95
2	Density (g/cm ³) (@ 30°C)	0.825	0.822	0.85 – 0.87
3	Viscosity (mm ² /sec) (@ 40°C)	2.90	2.60	1.9 – 4.5
4	Kinematic Viscosity (mm ² /sec) (@ 40°C)	3.438	3.163	1.9 – 4.8
5	pH	6.1	5.70	5.5 – 8.0
6	Flash Point (°C)	96.8	112.3	52 - 96
7	Pour Point (°C)	1.4	-5.3	-9.2
8	Refractive Index	1.483	1.522	1.460 – 1.462
9	Heating Value (MJ/kg)	32.218	42.114	41 – 46

CONCLUSION

Pre-degraded waste LDPE in toluene was pyrolyzed using thermal and catalytic methods to produce fuel-like liquids. When thermal pyrolysis was contrasted with catalytic pyrolysis, the former typically produced more oils than residue. This experiment produced a high yield of liquid products (about 72%) with promising physicochemical characteristics, as these attributes are comparable to the refinery's middle distillates. Additionally, according to GC-MS analysis, the liquid product formed by catalytic pyrolysis yielded roughly 70% of valuable compounds, whereas thermal pyrolysis produced 50%. This typically showed the effectiveness of the catalyst in the pyrolysis. Furthermore, if plastic waste conversions by cracking are to be ramped up to continuous operations, a dissolution process before degrading could also help prevent pipelines from clogging with melted plastic feed.

ACKNOWLEDGMENTS

The authors thank the Tertiary Education Trust Fund (TETFund) for providing the Institutional-Based Grant for this research.

REFERENCES

Agulló, J. C., Kumar, N., Berenguer, D., Kubička, D., Marcilla, A., Gómez, A. L., Salmi, T., & Murzin, D. Y. (2007). Catalytic pyrolysis of low density polyethylene over H-β, H-Y, H-Mordenite, and H-Ferrierite zeolite catalysts: Influence of acidity and structures. *Kinetics and Catalysis*, 48(4), 535–540. [\[Crossref\]](#)

Ahmad, I., Khan, M.I., Khan, H., Ishaq, M., Tariq, R., Gul, K., Ahmad, W., (2015). Pyrolysis study of polypropylene and polyethylene into premium oil products. *International Journal of Green Energy*, 12 (7): 663–671. [\[Crossref\]](#)

Akubo, K., Mohamad Anas Nahil, M. A. and Williams, P. T. (2019). Aromatic Fuel Oils Produced from the

Pyrolysis-Catalysis of Polyethylene Plastic with Metal-Impregnated Zeolite Catalysts. *Journal of the Energy Institute*, 92(1): 195-202. [\[Crossref\]](#)

American Society for Testing and Materials (ASTM) D56: Standard Test Method for Flash Point by Tag Open-Cup Tester. [cdn.standards.iteh.ai](https://www.astm.org/standards/D56)

American Society for Testing and Materials (ASTM) D1218 - Standard Test Method for Refractive Index and Optical Dispersion of Hydrocarbon Liquids). [cdn.standards.iteh.ai](https://www.astm.org/standards/D1218)

American Society for Testing and Materials (ASTM) D4739 - Standard Test Method for Determination of pH of Fuel Oil by Potentiometric Titration. [cdn.standards.iteh.ai](https://www.astm.org/standards/D4739)

ASTM Standard specification for biodiesel fuel (B100) blend stock for distillate fuels. In: Annual Book of ASTM Standards, ASTM International, West Conshohocken, Method D6751-08; 2008.

Bai, M., Song, Z., Yang, Z., Liu, Y., Qian, M., Zou, R., Lei, H., Zhang, Y., & Huo, E. (2022). Catalytic copyrolysis of low-density polyethylene (LDPE) and lignin for jet fuel range hydrocarbons over activated carbon catalyst. *International Journal of Energy Research*, 46(13), 18529–18539. [\[Crossref\]](#)

Barzallo, D., Lazo, R., Medina, C., Guashpa, C., Tacuri, C., & Palmay, P. (2023). Synthesis and Application of ZSM-5 Catalyst Supported with Zinc and/or Nickel in the Conversion of Pyrolytic Gases from Recycled Polypropylene and Polystyrene Mixtures under Hydrogen Atmosphere. *Polymers*, 15(16), 3329. [\[Crossref\]](#)

Budsareechai, S., Hunt, A. J., & Ngernyen, Y. (2019). Catalytic pyrolysis of plastic waste for the production of liquid fuels for engines. *RSC Advances*, 9(10), 5844–5857. [\[Crossref\]](#)

Burange, A. S., Gawande, M. B., Lam, F. L. Y., Jayaram, R. V., & Luque, R. (2015). Heterogeneously catalyzed strategies for the deconstruction of high density polyethylene: plastic waste

- valorisation to fuels. *Green Chemistry*, 17(1), 146–156. [\[Crossref\]](#)
- Damodharan, D., Kumar, B.R., Gopal, K., De Pours, M.V. and Sethuramasamyraja, B. (2019). Utilization of Waste Plastic Oil in Diesel Engines: A Review. *Reviews in Environmental Science and Bio/Technology*, 18: 681–697. [\[Crossref\]](#)
- Das, P. and Tiwari, P. (2018). Valorization of packaging plastic waste by slow pyrolysis. *Resources, Conservation & Recycling*, 128: 69–77. [\[Crossref\]](#)
- Doğan, Ö. M., & Kayacan, İ. (2008). Pyrolysis of low and high density polyethylene. Part II: Analysis of liquid products using FTIR and NMR spectroscopy. *Energy Sources. Part a, Recovery, Utilization, and Environmental Effects*, 30(5), 392–400. [\[Crossref\]](#)
- Ethiraj, J., Wagh, D., & Manyar, H. (2022). Advances in upgrading biomass to biofuels and oxygenated fuel additives using metal oxide catalysts. *Energy & Fuels*, 36(3), 1189–1204. [\[Crossref\]](#)
- Hasan, M. M., Batalha, N., Fraga, G., Ahmed, M. H., Pinard, L., Konarova, M., Pratt, S., & Laycock, B. (2022). Zeolite shape selectivity impact on LDPE and PP catalytic pyrolysis products and coke nature. *Sustainable Energy & Fuels*, 6(6), 1587–1602. [\[Crossref\]](#)
- Huang, H., Ye, X., Huang, W., Chen, J., Xu, Y., Wu, M., Shao, Q., Peng, Z., Ou, G., Shi, J., Xu, F., Feng, Q., Huang, H., Hu, P., & Leung, D. Y. (2015). Ozone-catalytic oxidation of gaseous benzene over MnO₂/ZSM-5 at ambient temperature: Catalytic deactivation and its suppression. *Chemical Engineering Journal (1996. Print)*, 264, 24–31. [\[Crossref\]](#)
- Huang, F., Yan, A., & Zhao, H. (2016). Influences of doping on photocatalytic properties of TiO₂ photocatalyst. In *InTech eBooks*. [\[Crossref\]](#)
- IEA (2023). World Energy Outlook 2023 Retrieved from iea.org on 15th May, 2023.
- Kaushal, J., Khatri, M., & Arya, S. K. (2021). Recent insight into enzymatic degradation of plastics prevalent in the environment: A mini - review. *Cleaner Engineering and Technology*, 2, 100083. [\[Crossref\]](#)
- Kholidah, N., Faizal, M., & Said, M. (2018). Polystyrene Plastic Waste Conversion into Liquid Fuel with Catalytic Cracking Process Using Al₂O₃ as Catalyst. *Science and Technology Indonesia*, 3(1), 1–6. [\[Crossref\]](#)
- Kim, Y. M., Lee, H. W., Choi, S. J., Jeon, J. K., Park, S. H., Jung, S. C., Kim, S. C., Park, Y. K. (2017). Catalytic co-pyrolysis of polypropylene and *Laminaria japonica* over zeolitic materials. *International Journal of Hydrogen Energy*, 42, 18434–18441. [\[Crossref\]](#)
- Kunwar, B., Moser, B.R., Chandrasekaran, S.R., Rajagopalan, N., & Sharma, B.K. (2016). Catalytic and thermal depolymerization of low value post-consumer high density polyethylene plastic. *Energy*, 111, 884–892.
- Li, C., Wu, H., Cen, Z. H., Han, W., Zheng, X., Zhai, J., Xu, J., Lin, L., He, M., & Han, B. (2023). Conversion of polyethylene to gasoline: Influence of porosity and acidity of zeolites. *Frontiers in Energy*, 17(6), 763–774. [\[Crossref\]](#)
- Li, N., Liu, H., Cheng, Z., Yan, B., Chen, G., & Wang, S. (2022). Conversion of plastic waste into fuels: A critical review. *Journal of Hazardous Materials*, 424, 127460. [\[Crossref\]](#)
- Liu, T., Li, Y., Zhou, Y., Deng, S., & Zhang, H. (2023). Efficient pyrolysis of Low-Density polyethylene for regulatable oil and gas products by ZSM-5, HY and MCM-41 catalysts. *Catalysts*, 13(2), 382. [\[Crossref\]](#)
- Mark, L. O., Cendejas, M. C., & Hermans, I. (2020). The use of heterogeneous catalysis in the chemical valorization of plastic waste. *ChemSusChem*, 13(22), 5808–5836. [\[Crossref\]](#)
- Mibe, Z., Kumar, A., & Talai, S. (2023). Catalytic pyrolysis of plastic waste to liquid fuel using local clay catalyst. *Journal of Energy*, 2023, 1–11. [\[Crossref\]](#)
- Nanakoudis, A. (2019). SEM: Types of electrons and the information they provide. ThermoFisher Scientific. [Thermofisher.com](http://thermofisher.com) Accessed 20 January, 2024.
- Quesada, L., Calero, M., Martín-Lara, M., Luzón, G., & Blázquez, G. (2020). Performance of different catalysts for the in situ cracking of the Oil-Waxes obtained by the pyrolysis of polyethylene film waste. *Sustainability*, 12(13), 5482. [\[Crossref\]](#)
- Rajan, K. P., Mustafa, I., Gopanna, A., & Thomas, S. P. (2023). Catalytic pyrolysis of waste Low-Density Polyethylene (LDPE) carry bags to fuels: Experimental and exergy analyses. *Recycling*, 8(4), 63. [\[Crossref\]](#)
- Roosbehani, B., Sakaki, S. A., Shishesaz, M., Abdollahkhani, N., & Hamedifar, S. (2015). Taguchi method approach on catalytic degradation of polyethylene and polypropylene into gasoline. *Clean Technologies and Environmental Policy*, 17(7), 1873–1882. [\[Crossref\]](#)
- Rouch, D. A. (2021) Plastic future: How to reduce the increasing environmental footprint of plastic packaging. Working Paper No. 11, Clarendon Policy & Strategy Group, Melbourne, Australia.
- Sarker, M., Rashid, M. M., Molla, M., & Rahman, M. S. (2013). Method of Converting Municipal Proportional Waste Plastics into Liquid Hydrocarbon Fuel by Using Activated Carbon. *International Journal of Materials and Chemistry*, 2(5), 208–217. [\[Crossref\]](#)
- Schyns, Z. O. G., & Shaver, M. P. (2020). Mechanical Recycling of Packaging Plastics: A review. *Macromolecular Rapid Communications*, 42(3). [\[Crossref\]](#)
- Seliverstov, E. S., Furda, L. V., & Lebedeva, O. E. (2022). Thermocatalytic Conversion of Plastics into Liquid Fuels over Clays. *Polymers*, 14(10), 2115. [\[Crossref\]](#)

- Setiawan, A., Setiani, V., & Mazdhatina, O. S. (2021). Characterization of fuel oil from pyrolysis waste light density polyethylene (LDPE) and polypropylene (PP). *IOP Conference Series. Materials Science and Engineering*, 1034(1), 012069. [\[Crossref\]](#)
- Shilpa, N., Basak, N., & Meena, S. S. (2022). Microbial biodegradation of plastics: Challenges, opportunities, and a critical perspective. *Frontiers of Environmental Science & Engineering*, 16(12). [\[Crossref\]](#)
- Song, J., Sima, J., Pan, Y., Lou, F., Du, X., Zhu, C., & Huang, Q. (2021). Dielectric Barrier Discharge Plasma Synergistic Catalytic Pyrolysis of Waste Polyethylene into Aromatics-Enriched Oil. *ACS Sustainable Chemistry & Engineering*, 9(34), 11448–11457. [\[Crossref\]](#)
- UNIDO (2021). Study on plastic value-chain in Nigeria. Retrieved from unido.org on 28th November, 2023.
- Vichaphund, S., Aht-Ong, D., Sricharoenchaikul, V., & Atong, D. (2014). Catalytic upgrading pyrolysis vapors of Jatropha waste using metal promoted ZSM-5 catalysts: An analytical PY-GC/MS. *Renewable Energy*, 65, 70–77. [\[Crossref\]](#)
- Wong, S. L., & Abdullah, T. a. T. (2014). Study on Dissolution of Low Density Polyethylene (LDPE). *Applied Mechanics and Materials*, 695, 170–173. [\[Crossref\]](#)
- Wong, S., Ngadi, N., Abdullah, T. a. T., & Inuwa, I. M. (2015). Recent advances of feed-in tariff in Malaysia. *Renewable & Sustainable Energy Reviews*, 41, 42–52. [\[Crossref\]](#)
- Wong, S. L., Abdullah, T. a. T., & Inuwa, I. M. (2016). Catalytic cracking of LDPE dissolved in benzene using Nickel-Impregnated zeolites. *Industrial & Engineering Chemistry Research*, 55(9), 2543–2555. [\[Crossref\]](#)
- Wong, S. L., Abdullah, T. a. T., & Inuwa, I. M. (2017). Conversion of low density polyethylene (LDPE) over ZSM-5 zeolite to liquid fuel. *Fuel*, 192, 71–82. [\[Crossref\]](#)
- Yao, D., Yang, H., Chen, H., & Williams, P. T. (2018). Investigation of nickel-impregnated zeolite catalysts for hydrogen/syngas production from the catalytic reforming of waste polyethylene. *Applied Catalysis. B, Environmental*, 227, 477–487. [\[Crossref\]](#)
- Zhang, S., Yang, M., Shao, J., Yang, H., Zeng, K., Chen, Y., Luo, J., Agblevor, F. A., & Chen, H. (2018). The conversion of biomass to light olefins on Fe-modified ZSM-5 catalyst: Effect of pyrolysis parameters. *Science of the Total Environment*, 628–629, 350–357. [\[Crossref\]](#)

APPENDIX

Table 3: Liquid phase GC-MS table of thermal pyrolysis of LDPE

PK	RT	Area Percentage (%)	Component	Chemical Formula
1	5.3037	0.0637	Benzene, 1-ethyl-3-methyl-	C ₉ H ₁₂
2	5.7392	0.7044	Toluene	C ₇ H ₈
3	5.9539	0.0453	1-Decene	C ₁₀ H ₂₀
4	6.7385	0.2824	4-Ethyl-2-hexynal	C ₈ H ₁₂ O
5	6.8241	0.1442	Phthalan	C ₈ H ₈ O
6	6.8471	0.1303	p-Cymene	C ₁₀ H ₁₄
7	6.9446	0.3334	D-Limonene	C ₁₀ H ₁₆
8	8.5792	0.1898	3-Phenylbut-1-ene	C ₁₀ H ₁₂
9	8.697	0.428	Cyclopropane, 1-heptyl-2-methyl-	C ₁₁ H ₂₂
10	14.4324	0.4671	1-Tridecene	C ₁₃ H ₂₆
11	14.5486	0.1062	1-Tridecene	C ₁₃ H ₂₆
12	14.6266	0.5916	Tridecane	C ₁₃ H ₂₈
13	16.0058	0.3667	1-Decanol, 2-hexyl-	C ₁₆ H ₃₄ O
14	17.3615	0.1313	Tetradecane	C ₁₄ H ₃₀
15	18.5928	0.5345	Hexacosanal	C ₂₆ H ₅₂ O
16	19.7655	0.0662	7-Hexadecene, (Z)-	C ₁₆ H ₃₂
17	19.9439	0.202	Pentadecane	C ₁₅ H ₃₂
18	20.4794	0.0116	1-Dodecanol, 2-hexyl-	C ₁₈ H ₃₈ O
19	22.3965	0.1034	Hexadecane	C ₁₆ H ₃₄
20	23.793	0.4687	Benzene, 1,1'-(1,3-propanediyl)bis-	C ₁₅ H ₁₆
21	24.3216	0.1508	Anthracene, 9,10-dihydro-9,10-dimethyl-	C ₁₆ H ₁₆
22	24.5686	1.2823	Trichloroacetic acid, pentadecyl ester	C ₁₇ H ₃₁ Cl ₃ O ₂
23	24.7037	0.6573	Heptadecane	C ₁₇ H ₃₆
24	26.8094	0.3709	1-Nonadecene	C ₁₉ H ₃₈
25	26.9537	1.1681	Octadecane	C ₁₈ H ₃₈
26	27.096	1.5672	Hexadecane, 2,6,10,14-tetramethyl-	C ₂₀ H ₄₂
27	28.7944	-0.0084	Octacosyl trifluoroacetate	C ₃₀ H ₅₇ F ₃ O ₂
28	28.8748	0.0539	Nonadecane	C ₁₉ H ₄₀
29	29.3059	0.1806	1-Bromodocosane	C ₂₂ H ₄₅ F
30	29.3542	0.0244	Cyclotetradecane, 1,7,11-trimethyl-4-(1-methylethyl)-	C ₂₀ H ₄₀
31	29.8145	6.9085	Di-sec-butyl phthalate	C ₁₆ H ₂₂ O ₄
32	29.9139	7.7372	1,2-Benzenedicarboxylic acid, butyl 2-methylpropyl ester	C ₁₆ H ₂₂ O ₄
33	29.9413	6.9057	Di-sec-butyl phthalate	C ₁₆ H ₂₂ O ₄
34	30.8785	0.3604	5-Methyl-Z-5-docosene	C ₂₃ H ₄₆
35	30.9272	0.1734	Cyclohexane, (1-hexyltetradecyl)-	C ₂₆ H ₅₂
36	30.9831	0.2083	Cyclotetradecane, 1,7,11-trimethyl-4-(1-methylethyl)-	C ₂₀ H ₄₀
37	31.3447	8.2902	Carbonic acid, but-2-yn-1-yl octadecyl ester	C ₂₃ H ₄₂ O ₃
38	32.011	12.0996	Tricosane	C ₂₃ H ₄₈
39	32.2195	0.3251	Triacontyl heptafluorobutyrate	C ₃₄ H ₆₁ F ₇ O ₂
40	32.2609	0.2414	Docosane	C ₂₂ H ₄₆
41	32.3559	0.6292	Carbonic acid, but-2-yn-1-yl eicosyl ester	C ₂₅ H ₄₆ O ₃
42	32.4203	0.2719	Ethanol, 2-(octadecyloxy)-	C ₂₀ H ₄₂ O ₂
43	32.7874	10.914	Tetratriacontyl heptafluorobutyrate	C ₃₈ H ₆₉ F ₇ O ₂
44	32.9754	0.6343	1-Decanol, 2-hexyl-	C ₁₆ H ₃₄ O
45	33.302	10.485	Tetratriacontyl heptafluorobutyrate	C ₃₈ H ₆₉ F ₇ O ₂
46	33.7236	1.9542	Octatriacontyl pentafluoropropionate	C ₄₁ H ₇₇ F ₅ O ₂
47	33.7464	0.2901	Carbonic acid, but-2-yn-1-yl eicosyl ester	C ₂₅ H ₄₆ O ₃
48	33.9655	7.5302	Tricosane	C ₂₃ H ₄₈
49	34.7107	0.4532	Carbonic acid, but-2-yn-1-yl eicosyl ester	C ₂₅ H ₄₆ O ₃
50	35.1989	6.8918	Octadecanoic acid, 17-oxo-, methyl ester	C ₁₉ H ₃₆ O ₃
51	36.011	0.3075	Tricosane	C ₂₃ H ₄₈
52	36.0742	0.0901	1-Docosene	C ₂₂ H ₄₄
53	36.5392	5.481	Silane, trichlorooctadecyl-	C ₁₈ H ₃₇ Cl ₃ Si
	Total	100		

Table 5: Liquid phase GC-MS table of catalytic pyrolysis of LDPE using Ni-ZSM-5

PK	RT	Area Percentage (%)	Component	Chemical Formula
1	6.0747	0.1146	1-Decene	C ₁₀ H ₂₀
2	21.5128	0.1727	17-Pentatriacontene	C ₃₅ H ₇₀
3	23.4874	0.308	Octacosyl trifluoroacetate	C ₃₀ H ₅₇ F ₃ O ₂
4	24.4639	0.2899	Dotriacontyl heptafluorobutyrate	C ₃₆ H ₆₅ F ₇ O ₂
5	26.2839	0.4481	Octacosyl trifluoroacetate	C ₃₀ H ₅₇ F ₃ O ₂
6	27.2674	0.8668	Carbonic acid, octadecyl prop-1-en-2-yl ester	C ₂₂ H ₄₄ O ₃
7	28.3323	0.7308	Triacetyl pentafluoropropionate	C ₃₃ H ₆₁ F ₅ O ₂
8	28.9047	0.9702	Octacosyl trifluoroacetate	C ₃₀ H ₅₇ F ₃ O ₂
9	29.327	1.2917	Octacosyl trifluoroacetate	C ₃₀ H ₅₇ F ₃ O ₂
10	29.528	1.0381	Tetraoctadecyl trifluoroacetate	C ₃₆ H ₆₉ F ₃ O ₂
11	29.8935	1.2369	Tetraoctadecyl trifluoroacetate	C ₃₆ H ₆₉ F ₃ O ₂
12	29.9927	1.1228	Diethyl Phthalate	C ₁₂ H ₁₄ O ₄
13	30.0408	0.8709	Diethyl Phthalate	C ₁₂ H ₁₄ O ₄
14	30.0916	1.343	9-Tricosene, (Z)-	C ₂₃ H ₄₆
15	30.2389	1.4313	1-Nonadecene	C ₁₉ H ₃₈
16	30.3353	1.1413	1-Nonadecene	C ₁₉ H ₃₈
17	30.5646	1.316	1-Docosene	C ₂₂ H ₄₄
18	30.7176	1.5531	1-Nonadecene	C ₁₉ H ₃₈
19	30.8595	1.4175	1-Nonadecene	C ₁₉ H ₃₈
20	30.9405	1.2237	1-Nonadecene	C ₁₉ H ₃₈
21	31.0619	1.3104	1-Nonadecene	C ₁₉ H ₃₈
22	31.1921	1.531	1-Docosene	C ₂₂ H ₄₄
23	31.2559	1.1728	1-Nonadecene	C ₁₉ H ₃₈
24	31.3748	1.4486	1-Nonadecene	C ₁₉ H ₃₈
25	31.4505	1.277	1-Docosene	C ₂₂ H ₄₄
26	31.564	1.4375	1-Heptadecene	C ₁₇ H ₃₄
27	31.6441	1.2963	1-Nonadecene	C ₁₉ H ₃₈
28	31.747	1.3932	1-Docosene	C ₂₂ H ₄₄
29	31.8358	1.3968	1-Octadecene	C ₁₈ H ₃₆
30	31.9088	1.2767	1-Tetradecene	C ₁₄ H ₂₈
31	32.0086	1.4327	5-Methyl-Z-5-docosene	C ₂₃ H ₄₆
32	32.0775	1.4204	1-Decanol, 2-hexyl-	C ₁₆ H ₃₄ O
33	32.1309	1.3737	9-Undecenal, 2,10-dimethyl-	C ₁₃ H ₂₄ O
34	32.1629	0.9769	1-Heptadecene	C ₁₇ H ₃₄
35	32.2697	1.1676	1-Nonadecene	C ₁₉ H ₃₈
36	32.3386	1.4593	Octadecane, 1-(ethenyl)-	C ₂₀ H ₄₀ O
37	32.3933	1.327	1-Bromo-11-iodoundecane	C ₁₁ H ₂₂ BrI
38	32.4352	1.1782	.alpha.-[p-Chlorophenyl]succinic acid	C ₁₀ H ₉ ClO ₄
39	32.4931	1.252	1-Eicosene	C ₂₀ H ₄₀
40	32.5282	0.2345	1-Docosene	C ₂₂ H ₄₄
41	32.5836	1.1581	Docosane	C ₂₂ H ₄₆
42	32.6459	1.3875	Tridecanedial	C ₁₃ H ₂₄ O ₂
43	32.6915	1.3292	1,2-Oxathiane, 6-dodecyl-, 2,2-dioxide	C ₁₆ H ₃₂ O ₃ S
44	32.7186	0.9614	1-Tetradecene	C ₁₄ H ₂₈
45	32.7933	1.2608	1-Pentadecene	C ₁₅ H ₃₀
46	32.8284	0.3198	1-Docosene	C ₂₂ H ₄₄
47	32.8901	1.3892	Hexacosane	C ₂₆ H ₅₄
48	32.915	0.9716	1-Decanol, 2-hexyl-	C ₁₆ H ₃₄ O
49	32.9521	1.1199	Cyclooctane, 1,5-dimethyl-	C ₁₀ H ₂₀
50	33.0099	1.4411	2-Heptadecenal	C ₁₇ H ₃₂ O
51	33.0368	0.9376	2-Heptadecenal	C ₁₇ H ₃₂ O
52	33.1116	1.2798	1-Nonadecene	C ₁₉ H ₃₈
53	33.1442	0.3401	Tricosane	C ₂₃ H ₄₈
54	33.2136	1.3768	Hexacosane	C ₂₆ H ₅₄
55	33.2428	0.9577	Tetrapentacontane, 1,54-dibromo-	C ₅₄ H ₁₀₈ Br ₂
56	33.3006	1.3656	1,22-Docosanediol	C ₂₂ H ₄₆ O ₂
57	33.3808	1.3789	Tetracosane	C ₂₄ H ₅₀
58	33.4393	1.3507	2-Heptadecenal	C ₁₇ H ₃₂ O
59	33.4818	1.1913	Ethanol, 2-(tetradecyloxy)-	C ₁₆ H ₃₄ O ₂
60	33.5567	1.2834	1-Heptadecene	C ₁₇ H ₃₄
61	33.646	1.5743	2-Heptadecenal	C ₁₇ H ₃₂ O
62	33.691	1.3092	.alpha.-[p-Chlorophenyl]succinic acid	C ₁₀ H ₉ ClO ₄
63	33.7294	1.0596	1-Decanol, 2-hexyl-	C ₁₆ H ₃₄ O
64	33.8354	1.3444	1-Docosene	C ₂₂ H ₄₄

Continued next page

Table 5 (Continued)

PK	RT	Area Percentage (%)	Component	Chemical Formula
65	33.9215	1.5742	1H-Cyclopenta[c]furan-1-one, hexahydro-3,6,6-trimethyl-	C ₁₀ H ₁₆ O ₂
66	33.9954	1.4655	Tetracosane	C ₂₄ H ₅₀
67	34.0356	1.0458	1-Eicosene	C ₂₀ H ₄₀
68	34.133	1.4087	1-Hexacosene	C ₂₆ H ₅₂
69	34.238	1.5087	1-Decanol, 2-hexyl-	C ₁₆ H ₃₄ O
70	34.288	1.1241	1-Hexacosene	C ₂₆ H ₅₂
71	34.4328	1.2244	1-Docosene	C ₂₂ H ₄₄
72	34.5324	1.5065	1-Decanol, 2-hexyl-	C ₁₆ H ₃₄ O
73	34.6439	1.6337	1-Nonadecene	C ₁₉ H ₃₈
74	34.688	0.9744	1-Nonadecene	C ₁₉ H ₃₈
75	34.8462	1.3722	1-Nonadecene	C ₁₉ H ₃₈
76	35.0328	1.6627	1-Nonadecene	C ₁₉ H ₃₈
77	35.1017	1.0678	Nonacos-1-ene	C ₂₉ H ₅₈
78	35.2766	1.7096	1-Nonadecene	C ₁₉ H ₃₈
79	35.3511	1.154	Heptacos-1-ene	C ₂₇ H ₅₄
80	35.4791	1.3943	Heptacos-1-ene	C ₂₇ H ₅₄
81	35.5916	1.0839	1-Nonadecene	C ₁₉ H ₃₈
82	35.802	1.5371	Nonacos-1-ene	C ₂₉ H ₅₈
83	36.1839	1.2209	Hexatriacontyl pentafluoropropionate	C ₃₉ H ₇₃ F ₅ O ₂
84	36.595	1.0975	Dotriacontyl heptafluorobutyrate	C ₃₆ H ₆₅ F ₇ O ₂
85	36.8891	0.8963	Tricosane	C ₂₃ H ₄₈
	Total	100		